Journal of Physics B: Atomic, Molecular and Optical Physics

Elastic Electron scattering by thermal mixture of glycine conformers in gas phase

OPEN ACCESS
IOP Publishing
Journal of Physics B: Atomic, Molecular and Optical Physics
J. Phys. B: At. Mol. Opt. Phys. **56** (2023) 045201 (12pp)
https://doi.org/10.1088/1361-6455/aca734

Elastic Electron scattering by thermal mixture of glycine conformers in gas phase

Mylena H Ribas[1], **Jonathan Tennyson**[2,*] **and Milton M Fujimoto**[1,*]

[1] Departamento de Física, Universidade Federal do Paraná, 81531-990 Curitiba, PR, Brazil
[2] Department of Physics & Astronomy, University College London, Gower St., London WC1E 6BT, United Kingdom

E-mail: j.tennyson@ucl.ac.uk and milton@fisica.ufpr.br

Received 17 September 2022, revised 2 November 2022
Accepted for publication 29 November 2022
Published 3 February 2023

Abstract

A theoretical study of electron scattering by a thermal mixture of glycine molecules in the energy range from 1 to 10 eV is performed using the UK-RMol codes which are based on the R-Matrix method. The six lowest relative Gibbs free energies glycine conformers considered, Ip, IIp, IIn, IIIp, IIIn and IVn, are significantly populated in thermal mixtures. All these conformers present similar resonance structures in the eigenphase sums: a lower-energy resonance state near 1.8 eV and another at higher-energy above 7 eV. For the six conformers the lowest resonance lies between 1.75 eV and 2.21 eV. The very large dipole moments of 6.32 D and 5.67 D for IIp and IIn, respectively, makes the magnitude of their cross sections significantly larger than other conformers, which increases the average cross sections in thermal mixtures compared with the cross sections of the lowest energy Ip conformer. Three conformer population sets are used to calculate the averaged differential and integral cross sections: two theoretical sets based on the relative Gibbs free energies and another set that aims to mimic experiment based on the observed populations. The averaged cross sections are similar for all population sets, but differ from the Ip conformer cross section. This suggests that, for large and flexible molecules, the computed average cross sections should be used when comparing with experimental data.

Keywords: elastic, electron, scattering, thermal, mixtures, glycines

(Some figures may appear in colour only in the online journal)

1. Introduction

Since the discovery that slow electrons (<20 eV) can damage plasmid DNA [1] studies of low-energy electron scattering by molecules of biological interest has increased hugely. This issue is relevant when ionizing radiation hits living tissue producing large quantities of secondary, low-energy electrons. The general mechanism proposed to shatter DNA molecules goes through the formation of a temporary anion states (resonance) which decay into fragments via dissociative electron attachment (DEA). In the shape resonance, the transient negative ion (TNI) is formed when a low-energy electron is captured by an unoccupied target orbital. If this metastable state crosses the target state potential, it is possible that the molecule decays into fragments. To understand the fragmentation complex dynamics many experimental and theoretical studies of DNA constituents are found in the literature using precursor organic molecules, nucleobases, amino acids, sugar backbone, phosphates, etc see Sanche [2] and references therein.

* Authors to whom any correspondence should be addressed.

The glycine molecule is the simplest, non-essential and proteinogenic amino acid; it is a precursor which is incorporated into proteins biosynthetically. This flexible molecule has three internal rotational degrees of freedom associated with the C–C, C–N, and C–O bonds, see figure 1, which lead to the formation of several stable conformers. Glycine is observed in zwitterionic form in the condensed phase (crystalline or in solution) [3, 4], however the gaseous glycine conformers exist in neutral (non-zwitterionic) form [5–8]. Neutral glycine also provides a good model to understand more complex biomolecules such as peptides, proteins or even DNA. Glycine is a solid powder at room temperature. To observe rotational and vibrational spectra, and to make electron scattering measurements in the gas phase, it is necessary to warm up the substance to near 150 °C; many theoretical studies indicate that there are manifold stable conformers with relative energies lower than 1000 cm^{-1} therefore is expected that several conformers will coexist in glycine vapour.

The significance of gaseous glycine conformers can be evidenced in a pertinent discussion in the literature. In 1977, Vishveshwara and Pople [9] calculated optimized structures of glycine conformers using standard bond lengths and angles at the Hartree–Fock (HF) level with 4-31G basis sets and found two stable conformers: stretched form I (lowest-energy) and a cyclic form II. In 1978, two independent measurements of microwave (MW) spectrum of glycine [10, 11] assigned a conformer where the rotational constants and the dipole moment were in conflict with the lowest-energy structure for glycine proposed by Vishveshwara and Pople. Brown *et al* [11] declared that glycine vapour could contain more than one conformer. They inferred that the detected cyclic form was the lowest energy conformer because they assumed that it was the most abundant form. This misunderstanding started to be resolved when Sellers and Schäfer [12] performed full geometry optimization calculations for glycine structures and confirmed that the lowest-energy conformer was the stretched form I in agreement with Vishveshwara and Pople. They found a small energy difference between the conformers I and II of 2.2 kcal mol^{-1}. The dipole moment of the cyclic structure II is 6.5 D which is consistent with the high experimental molecular dipole moment observed for structure II along the *a* inertial axis of 4.6 D, in MW spectra [11]. Since the dipole moment of the conformer I is much smaller, near 1.1 D, they also concluded that theoretical results did not necessarily contradict the experiments and species I and II could both exist in the vapour, but that conformer I would give relative weak intensities in the MW as the intensities of pure rotational transitions are proportional to the square of the dipole moment. This means that even in an Boltzmann equilibrium distribution of mixture of conformers, the MW spectrum could be dominated by the less populated conformer (glycine II). Reconciliation between theory and experiment came when new spectra of gaseous glycine detected a new conformer (I) with relative energy below the previously reported conformer (II) [5, 6, 13, 14]. The resulting experimental spectroscopic parameters are in reasonable agreement with the theoretical calculations.

A related issue is the relative population of conformers in glycine vapour. As the MW/millimeter spectra of glycine are strongly dependent on the dipole moment, the transition intensities alone cannot be used to estimate the relative population, as some conformers have relatively large dipoles and therefore even when less populated can give a strong signal. An alternative approach to getting the relative populations is to use theory to find reliable energy differences between conformers. However, achieving the accuracy required to give the composition in a thermal mixture is a challenging task for both theory and experiment. Some disagreement in geometric structures, proposed by spectral analysis and calculations, prompted many theoretical searches of the potential energy surface (PES) to find optimized geometries and molecular properties for stable, non-zwitterionic glycine conformers [15–30]. Conformational features and stable geometries in the gas phase are determined by internal interactions which are related to bond rotations, steric strain, steric repulsion of electron lone-pairs and intramolecular hydrogen bond. The last one is the dominant intramolecular factor in stabilizing various conformers [23, 31, 32]. So a high accuracy description of these effects is required to determine the fidelity of the relative energies theoretically. Both the use of high level methods and the choice of basis set are important. To obtain correct conformer structures methods which treat electron correlation are necessary (MP2, MP4, CISD, CCSD(T), DFT) as also large polarised and diffuse basis sets, see [7, 17, 24, 25, 29, 30, 33, 34] and references therein. For example, Császár [27] performed correlated level *ab initio* calculations for 13 conformers of neutral glycine obtaining accurate geometric structures and various properties of spectroscopic interest. His calculations at the corrected B2 MP2 level showed that the six lowest energies conformers, Ip, IIp, IIn, IIIp, IIIn and IVn, should be the most populated. B2 is a large basis set [27]. In Császár's notation 'p' refers to a planar configuration of heavy atoms (N–C–C–O) and 'n' refers to non-planar. Independent of the method or basis set used all theoretical predictions point to the Ip as the lowest-energy conformer and this conformer should be the most populated conformer at any temperature.

From the experimental point of view, many studies used theoretical rotational constants and transition frequencies in attempts to identify glycine conformers in thermal mixtures. Besides the MW spectra cited above, gas phase electron diffraction was applied to evaluate relative energies between conformer I and II, and estimate a population of 76% and 24% at temperature of 219 °C, respectively [6]. Jet expansion spectroscopic investigations found that only conformers I and II were observed after expansion [35, 36] in proportion 79% to 21%, which are in contrast with their theoretical calculations which predicted that the lowest four (I, II, IV and VII) conformers should be present in detectable amounts. A possible explanation is that while a 219 °C Boltzmann equilibrium distribution was used in the jet expansion, during the expansion collisional relaxation occurs to conformers I and II, facilitated by the low barrier of interconversion (for example, IV → I). A few experiments using noble gases (Ar, Ne, Kr) matrix-isolation combined with Fourier transform infrared spectroscopy allowed conformers I, II and III to be observed [37–39]. The relative population in a glycine thermal mixture is a complex issue and some authors suggest that it does not depend only on relative

energies but also on other factors such as quantum effects or dynamical of interconversion due to absence of direct pathway [28, 34].

All of this issues have significance for any comparison between theory and experiment of electron collision cross sections for gas-phase glycine. There are some studies involving electron scattering by neutral glycine molecules in gas phase. Iijima *et al* [6] made a joint analysis of electron diffraction and rotational constants indicated the presence of more than one glycine conformer in 219 °C vapour and proposed geometric parameters for the glycine conformer which generated the most intense signal observed. Neville *et al* [40] using momentum profiles (orbital images) of gaseous glycine from electron momentum spectroscopy measurements and electronic structure calculations proposed the presence of the five lowest energy conformers (Ip, IIp, IIIp, IVn, and Vn) which were Boltzmann weighted at 165 °C. Aflatooni *et al* [41] measured the TNI formation of some amino acids by the electron transmission spectroscopy and reported vertical attachment energy. They assigned the experimental value of 1.93 eV to the attachment of electron to π^* orbital of –COOH group of glycine molecule. DEA of glycine provided the most prominent peaks, around 1.2–1.4 eV associated with the fragmentation of the $[G–H]^-$ anion and also above 5.5 eV [42–46]. Gianturco and Lucchese [47] studied three glycine conformers and reported resonance spectra and possible anions states involved in fragmentation of the molecule. Tashiro [48] and dos Santos *et al* [49] reported theoretical elastic cross sections for glycine. dos Santos *et al* also analysed the resonance feature for the second conformer of glycine. Although some of the above works comment on the possibility of the existence of glycine conformers, only actually consider the lowest energy conformer in the analysis of their data. We are proposing a systematic analysis of the contribution of the most populated glycine conformers in a thermal mixture to the resonance features and the elastic scattering cross sections.

In this work we present elastic electron collision cross section for six conformers of glycine and a thermal mixture of these conformers computed using R-Matrix method. First, we compare our cross section for each conformer with the lowest energy conformer Ip. Then we simulate the cross sections of thermal mixtures of glycine conformers. This paper is organised as follows: section 2 presents details of calculation and the R-Matrix methodology used; section 3 results and discussions are presented. Section 4 presents our concluding remarks and summarizes the present findings.

2. Calculation details

2.1. R-matrix method

The UK molecular R-matrix methodology used in this work is described in detail in [50, 51], and the references therein. We present the most relevant features of the method.

In this method, the configuration space is divided in two regions: inner and outer. The inner region is delimited by a sphere of radius a which should contain all the electronic density of the N-electrons of the isolated target. In this region, a complex of $N+1$ electrons is formed and the continuum electron has short-range interactions, and the correlation and exchange interactions must be described more precisely than in the outer region. The inner region is the most demanding in terms of computational time and effort however the advantage in this step is that the electronic structure of the $(N+1)$-electron complex needs to be calculated only once for each symmetry.

In the inner region, the $(N+1)$-electron wave function is described by

$$\Psi_k^{N+1}(x_1 \ldots x_{N+1}) = \mathcal{A} \sum_{ij} a_{ijk} \phi_i^N(x_1 \ldots x_N) u_{ij}(x_{N+1}) + \sum_i b_{ik} \chi_i^{N+1}(x_1 \ldots x_{N+1}) \quad (1)$$

where ϕ_i^N is the target wave functions of the ith state; u_{ij} represents the continuum electron orbital; $\mathcal{A}$ is the antisymmetrization operator due to the indistinguishability of inner-region electrons that must satisfy the Pauli principle. The second summation in equation (1) depict functions χ_i^{N+1} which describe all $N+1$ electrons but should vanish at $r=a$; these are described by L^2 configurations and are added to relax the constraint of orthogonalization between continuum and target orbitals of the same symmetry, and, as discussed below, to simulate the polarisation of the electronic cloud of the target; a_{ijk} and b_{ik} are the variationally-optimized coefficients of expansions. The partial wave expansion is used to expand the target and continuum orbitals, consequently, also interaction potential and K-matrix, up to some maximum value of $\ell = \ell_{\max}$ where we consider the reasonably converged results.

In a static-exchange (SE) calculation the continuum electron is allowed to occupy a virtual (unoccupied target) orbital. Polarisation effects are included in the inner region via second sum in equation (1), using singly-excited L^2 configurations of the HF ground state wave function. Each configuration is obtained by promoting one target electron into a virtual orbital and also the continuum electron into a virtual orbital generating a two-particle one-hole (2p,1h) configuration. This model of calculation is called static-exchange plus polarisation (SEP) level. The polarisation level is handled by the number of virtual orbitals (NV) considered to generate the L^2 configurations.

In the outer region, the interaction of the continuum electron with the N-electron target is weaker than in the inner region; it can be represented via long-range multipole potential interactions, such as dipole interactions, and it is not necessary to explicitly include correlation and exchange effects. In this region, the scattering electron is described by one-electron wave function which moves in an scattering potential computed by the electronic density of the target. A one-particle coupled second-order differential equation for the continuum electron is solved for the electron scattering process. The inner and outer solutions are match by the R-matrix on the sphere boundary. The R-matrix is propagated to large r where the K-matrices and scattering observables are computed.

Glycine molecule has a permanent dipole, so the Born closure procedure is used to take into account a portion of long-range interaction that is neglected when partial waves from 0

to ℓ_{max} are considered. To include higher partial waves, our ℓ_{max} T-matrices are added to analytic dipole Born T-matrices, using the ANR approximation to take account of rotational motion, and then corrected by subtracting the partial wave dipole Born contributions [52–54]. To avoid the divergence of nuclei fixed approximation in forward direction we are using rotating dipole approximation to include rotational motion in the Born closure procedure [52]. The rotationally-unresolved elastic differential cross sections are obtained by the sum of rotationally-resolved elastic and inelastic cross sections until convergence. All these calculations are performed with the code POLYDCS [55] and only the rotationally-unresolved cross sections are presented here.

In this work, initial input files were generated using version 4.1 of the Quantemol-N expert system [56], and calculations at the SEP level are performed directly with the UKRMol codes [57]. Quantemol-N provides a quick way to construct correct and self-consistent inputs for the UKRMol code at the SE level which we adjust to perform SEP calculations.

Convergence analysis of the R-Matrix calculations followed our previous work [58], where we tested parameters such as: radius a from 10 to 15 a_0; ℓ_{max} equal 4 and 5. And the numbers of virtual orbitals (NV) up to 50. For all results presented, values adopted here are: $a = 10\ a_0$; $\ell_{max} = 4$ and $NV = 40$. These parameters were chosen based on reasonable convergent results and computational cost. For example, the ICS changes less than 2% when we move from $NV = 40$ to $NV = 50$ in an SE level calculation.

2.2. Conformers

Császár's [27] PES search found altogether 13 conformers of non-zwitterionic glycine which are all expected to exist in gas phase; no glycine conformers are expected to coexist in equilibrium in the gas phase in the zwitterionic form. Here we only consider the six lowest energy conformers from Császár's calculations, because we assume they will contribute more significantly to the thermal population. These conformers are Ip, IIp, IIn, IIIp, IIIn, IVn and their structures can be seen in the figure 1. The order of energies for these six lowest relative energies conformers were confirmed by Ke *et al* [29] who calculated also relative Gibbs free energies at 298 K. The conformer populations at a given temperature are better estimated using relative Gibbs free energies instead of relative energies, which we used in our previous study of α-alanine [59].

Our calculations used HF level target wavefunctions computed with 6-311G** or cc-pVTZ basis sets. However, as the cross sections proved to be very similar, all the data presented in this paper were calculated using 6-311G** basis set. The geometries used in this work were optimized by Császár [27] and we are following the same nomenclature used in that work. Even though the 'p' conformers can be represented by the C_s point group while 'n' conformers have no symmetry (C_1 point group), in this comparative study we decided to represent all conformers using the C_1 point group to ensure the same R-Matrix parameters for all conformers, unless specified otherwise.

To represent the thermal mixture of glycine conformers at a given temperature, three population sets are considered, two theoretical and one experimental, are presented in table 1. The first theoretical population set for Ip, IIp, IIn, IIIp, IIIn and IVn glycine conformers is determined by the Boltzmann equilibrium ratio using the relative Gibbs free energies at 298 K from Ke *et al* [29] calculated in the B3LYP/6-31+G*. The other theoretical set is obtained from relative Gibbs free energies at 438 K calculated by Neville *et al* [40], who deemed that Ip, IIp, IIIp, IVn and Vn should be present in significant amount. Neville *et al*, based on previous experiments which did not observe some of the conformers predicted by calculation and also in their own theoretical results, proposed a population set with only five conformers. However, as shown in table 1, we consider only the Ip, IIp, IIIp and IVn conformers to represent the population set of Neville *et al* [40], since the Vn conformer should contribute only around 1.6% at 438 K and its dipole moment is intermediary, near 2.4 D. Therefore we do not expect that Vn would contribute significantly to the averaged cross sections. In addition to the different conformer composition and temperature between [29, 40], we can attribute part of the difference in proportion of the IIp and IIIp conformers in the two sets to the DFT functionals used to estimate the free Gibbs energies. For example, Ke *et al* [29] observed the functional PBE1PBE resulted in different relative Gibbs free energies compared to the B3LYP functional and consequently to the different populations. The experimental population set was obtained from Stepanian *et al* [38] who observed only three conformers in the matrix isolation in inert gases; these conformers were assigned as I, II and III, and belonging to point groups C_s, C_1 and C_1, respectively. Stepanian *et al* evaporated the glycine at temperature of 170 °C (443 K) and then converted the vapour into a matrix isolation to probe the existence of these three conformers. As they do not identify the conformers in 'p' and 'n' configurations, to calculate the averaged cross sections we supposed, for example, the population of conformer II and III are distributed in the same proportion of n and p that we have estimated the population at 443 K using data from Ke *et al*.

3. Results and discussion

3.1. Eigenphase sums for conformers

The eigenphase sums for the six Ip, IIp, IIn, IIIp, IIIn and IVn glycine conformers are presented in the figure 2. All results are at the SEP level with $NV = 40$ virtual orbitals including a Born correction. The resonance positions and widths were fitted by an automated procedure [60] using the Breit–Wigner formula. Table 2 shows the resonance positions and widths found for the six glycine conformers. Some very narrow resonance states for energies above 6 eV are not listed; these are likely pseudo-resonance and artifacts of the calculation procedure.

As shown in figure 2 the eigenphase sums for all conformers exhibit two resonance structures, one at lower energy near 1.9 eV and another at higher energies near 8 eV. The lower-energy shape resonance ranges from 1.75 eV, for IIIn,

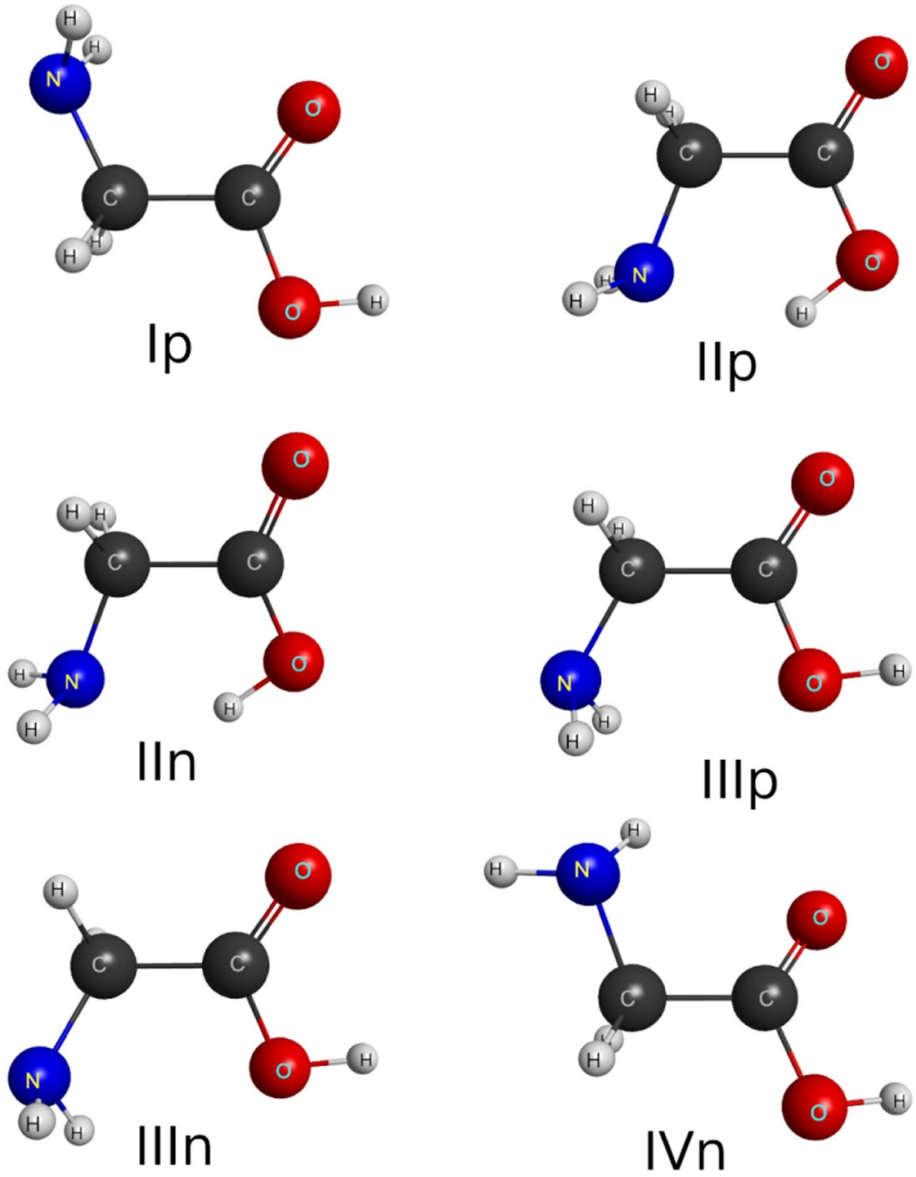

Figure 1. Structure of six lowest-energy gas-phase conformers of glycine: Ip, IIp, IIn, IIIp, IIIn and IVn. The figures were obtained using MacMolPlot [64].

Table 1. Theoretical and experimental population, in %, of glycine conformers at temperatures of 298 K, 438 K and 443 K, respectively. The theoretical values are based on relative Gibbs free energies from Ke *et al* [29] and Neville *et al* [40]. The experimental data are estimated from Stepanian *et al* [38].

Theoretical				Experimental	
$T = 298$ K		$T = 438$ K		$T = 443$ K	
Conformer	Population [29]	Conformer	Population [40]	Conformer	Population [38]
Ip	62.6	Ip	53.7	I	70
IIp	4.50	IIp	9.1	II	15
IIn	12.60	—	—		
IIIp	8.40	IIIp	30.2	III	15
IIIn	8.69	—	—		
IVn	3.21	IVn	6.9	—	—

up to 2.21 eV for IIp conformer. The most stable conformer Ip displays this feature at 1.82 eV. This shape resonance is referred in literature as being due to the electron attachment in the unoccupied π^* orbital of CO bond, it has been observed in molecules with –COOH group, such as amino acids. Aflatooni *et al* [41] using electron transmission

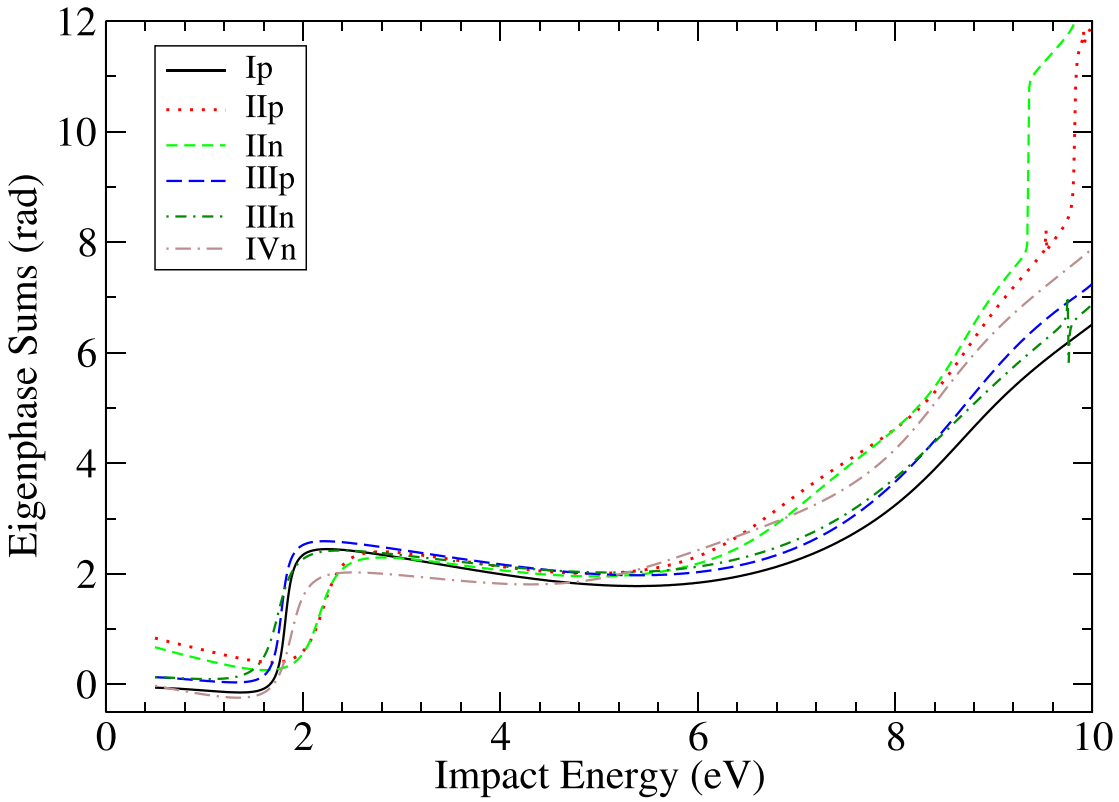

Figure 2. SEP eigenphase sums for electron scattering by the six lowest-energy gas-phase conformers of glycine: Ip, IIp, IIn, IIIp, IIIn and IVn.

Table 2. Resonance Position (P) and Width (W), in eV, for the six lowest energy conformers of glycine. Dipole moments are in Debye.

Conformer	Dipole	P	W	P	W	P	W	P	W
Ip	1.23	1.82	0.12	8.71	1.68				
IIp	6.32	2.21	0.33	7.13	2.01	8.67	2.08	8.80	1.19
IIn	5.67	2.17	0.34	7.59	2.12	8.72	0.97		
IIIp	2.00	1.78	0.13	8.69	1.66				
IIIn	1.91	1.75	0.27	8.67	2.23				
IVn	2.28	1.88	0.26	8.50	1.34				

spectroscopy measured the vertical electron attachment for the temporary anion formation for glycine as being 1.93 eV. These results are corroborated by other experiments studying vibrational excitation in the lowest-energy resonance region [45, 61]. Experimental studies on DEA of amino acids show a peak in the cross sections near 1.2 eV which, due to the proximity to the shape resonance, are widely attributed to attachment via the –COOH π^* orbital. However, Scheer *et al* [43] discuss the possibility that this 1.2 eV feature could be due to direct attachment to the lowest σ^* orbital.

On the theoretical side, only a few studies have calculated electron-scattering cross-sections and resonance positions. Tashiro [48], using the R-Matrix method, found the lower-energy resonance calculated at the SEP level at 2.15 eV. Although Tashiro performed calculations at other levels such as close-coupling studies with a CASSCF target wavefunctions, we are also using the SEP method; there are some differences between our calculation that could explain the discrepancy. First, Tashiro used a maximum of only $NV = 30$ virtual orbitals in his polarisation model and we use $NV = 40$ virtual orbitals, meaning that our treatment includes increased polarisation effects. Another difference is that the dipole moment for glycine molecule calculated by Tashiro is 1.95 D and our lowest-energy conformer Ip presents 1.23 D. It would appear that Tashiro performed calculations with a glycine structure closer to the IIIn or IIIp conformers (see the dipole moment at table 2). Another theoretical study on electron scattering was done by dos Santos *et al* [49] using the Schwinger Multichannel method (SMC) and obtained a π^* shape resonance position of 2.4 eV for the lowest energy conformer at the SEP level. It seems that the glycine molecular geometry used by dos Santos *et al* [49] should be similar to our Ip conformer as the dipole moment of their conformer is 1.317 D. Since in their method the polarisation potential is calculated like our method, part of the difference in the resonance position is probably due the level of polarisation included.

A broad structure is also seen in the eigenphase sums, in figure 2, for all conformers starting from 6 eV, which we call the higher-energy resonance region. Table 2 shows the higher-energy resonances ranging from 7.1 eV to 8.8 eV. This structure is also supplemented by some other narrow structures which are not presented in the table. This higher-energy

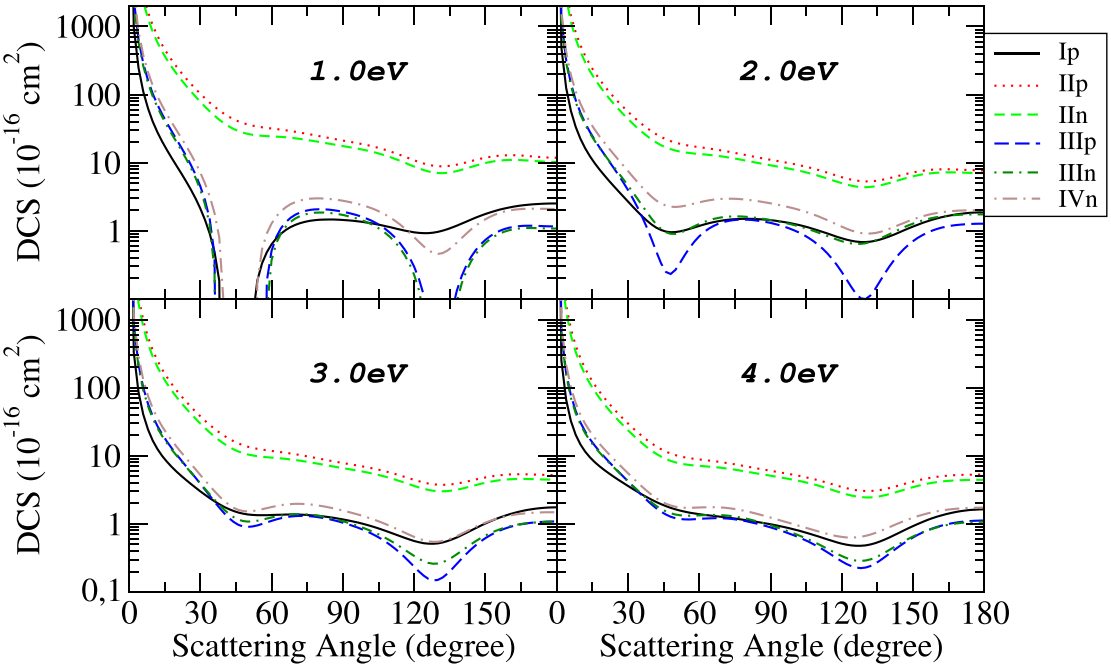

Figure 3. SEP differential cross sections with Born closure for electron scattering by glycine Ip, IIp, IIn, IIIp, IIIn and IVn conformers for impact energies of 1, 2, 3 and 4 eV.

resonance is more complex to assign to a specific process and in the literature it is generally described as to a core excited shape resonances [43, 48], which occurs when the continuum electron is attached to an electronically excited state of the target molecule. A DEA experimental study of gas phase glycine showed appearance of fragments, such as, $[\mathrm{Gly}-\mathrm{H}]^-$, $[\mathrm{H_4C_2NO}]^-$ and $[\mathrm{H_2C_2O_2}]^-$ at lower energies while were detecting many small fragments, for example, $[\mathrm{OH}]^-$, $[\mathrm{O}]^-/[\mathrm{NH_2}]^-$, $[\mathrm{HCO_2}]^-$, etc appearing at energies ranging from 6 eV to 8 eV [42]. Gianturco and Lucchese [47] made a theoretical study to understand the dynamics of resonant capture of low energy electrons and an analysis in the TNI to explain the DEA experiment. They plotted the wave functions of the resonant states for three glycine conformers in the plane of heavy atoms of the molecule to indicate some possible pathways of fragmentation. For higher-energy resonance states they observed that these very likely lead to core-excited shape-resonance trappings.

In general, for most conformers basically two resonance regions were found: lower-energy near 1.9 eV and a higher-energy with broad resonance around 8 eV. Except for the structures IIp (6.32 D) and IIn (5.67 D) which where the fits found four and three resonance states, respectively. These extra resonances are probably related to the strong permanent dipole moment in these two conformers. Dipole bound states could also be expected for these conformers, since their dipole moments are bigger than the critical value to support them (>1.625 D) [62]. In fact, the electron binding energy for dipole bond state was predicted and measured for conformer II anion formation (>5.5 D) [63]. However, in our R-Matrix calculation, for IIp conformer at $NV = 50$ level of polarisation, the total energy of the lowest-energy anion state remains just above zero.

3.2. *Differential cross sections for conformers*

Figures 3 and 4 present differential cross sections (DCSs) for glycine Ip, IIp, IIn, IIIp, IIIn and IVn conformers for impact energies of 1, 2, 3, 4, 5, 6, 8 and 10 eV. The calculations are done in SEP level ($NV = 40$) and the Born closure procedure used to account for higher partial waves. The electron scattering cross sections follow a similar trend to that discussed above for the MW spectrum, i.e. conformers with larger dipole moment have larger cross sections, as seen for IIp, IIn and IVn. At 1 eV, the cross sections of conformers are more sensitive for the details of molecular structure. The minimum near 45° and 135° indicates that the *d*-partial waves are dominant in DCS for impact energy below 5 eV, for all conformers. The deep minima seen at 1 eV, near 45 and also at 145° for Ip, IIIp and IIIn conformers, are artifacts caused by the combination of Born closure procedure and the polarisation level: this structure increases or disappears depending on the number of virtual orbitals considered in the SEP calculation. This behaviour is also observed for other methods in the literature when Born closure is used. In the DCS forward directions, as expected, the IIn, IIp and IVn conformers show large cross sections below 30° compared to Ip, due to their larger dipole moment.

As the impact energy increases all DCSs move closer to that to of the Ip conformer. For example, at 10 eV the DCS is much less sensitive to the spatial arrangement of group of atoms, mainly for Ip, IIIp, IIIn and IVn conformers. However

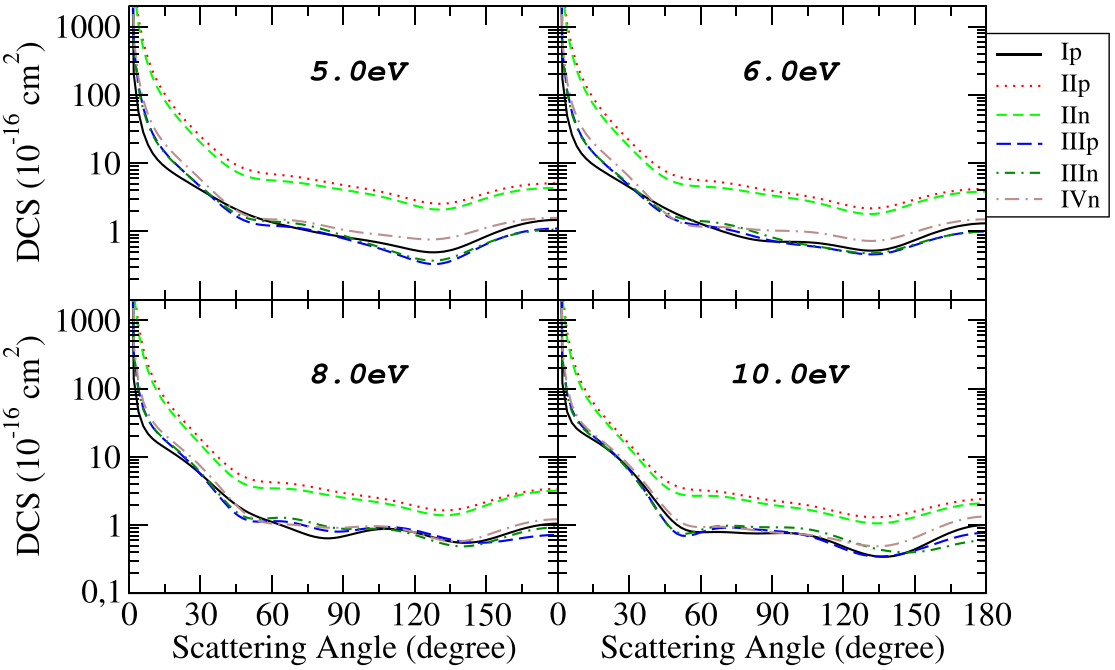

Figure 4. SEP differential cross sections with Born closure for electron scattering by glycine Ip, IIp, IIn, IIIp, IIIn and IVn conformers for impact energies of 5, 6, 8 and 10 eV.

the DCS for IIn and IIp are still bigger than Ip because of the large difference between their dipole moments.

3.3. Averaged DCS

The averaged differential (or integral, ICS) cross sections for the six lowest-energy conformers are weighted by the population ratio given by

$$(\mathrm{CS})^{\mathrm{avg}}(T) = \sum_i c_i(T)(\mathrm{CS})_i \qquad (2)$$

where $c_i(T)$ are the temperature-dependent equilibrium Boltzmann population ratios and $(\mathrm{CS})_i$ are the SEP DCS (or ICS) with Born closure for the ith conformer.

The DCS for a thermal mixture of gas phase glycine conformers are shown in the figures 5 and 6 and compared with the most stable conformer Ip and also with the only two theoretical DCS available for glycine. These two DCS data, one was calculated by Tashiro [48] using the R-Matrix method and another done by dos Santos *et al* [49] using the SMC method, both computed at the SEP level without Born closure, while our calculations for glycine Ip conformer and the averaged DCS (AVG-DCS) include Born closure and they reflect, in part, the difference in behaviour of DCS at small angles. One reason for the difficulty in making a straight comparison between our results for the Ip conformer with the DCS reported by [48, 49], is that neither of these studies disclosed the glycine geometries used in their calculations. The stated values of glycine dipole moment (1.95 and 1.317 D) suggest that the geometry used by Tashiro differs from that adopted by dos Santos *et al* [49]. Despite that, the DCS of [48, 49] are in reasonable magnitude agreement in the energy range shown. At 3 eV their DCS results are higher than ours for Ip which can be explained because there is a resonance near this energy in their calculations that could affect the magnitude of DCS, our lower-energy resonance is shifted to 1.82 eV. However, our DCS results for Ip is lower than those of Tashiro and dos Santos *et al* above 45° for all energies. At impact energies of 8 and 10 eV, the comparison with DCS from Tashiro and dos Santos *et al* with our results is surprising because their results are even larger than all our AVG-DCSs (AVG-teo1, AVG-teo2 and AVG-exp). As our AVG-DCS (teo1) includes contributions from conformers IIp and IIn which have very large dipole moments, this is unexpected. To understand this issue, we made some tests. First, we compared (not shown) the DCS for Ip for a SE calculation level with their available cross sections and find good agreement. However, the difference increases with the level of polarisation included. When we calculate the Ip conformer using C_s point group symmetry, the low-energy resonance feature appear in the $^2A''$ symmetry and the behaviour is the same as that observed in Tashiro and dos Santos *et al*'s cross sections. The discrepancy appears in the $^2A'$ partial symmetry which has no lower-energy resonance feature, however, in our calculation the introduction of polarisation effects reduces the cross sections in this symmetry. As our calculation has higher level of polarisation effects than Tashiro, it could partly explain the difference. Another part of this difference could be attributed to Born closure procedure.

The averaged DCS (AVG-DCS) was calculated using three population sets, two theoretical and one experimental. The first population set, named AVG-teo1, was derived from the relative Gibbs free energies for glycine Ip, IIp, IIn, IIIp, IIIn and

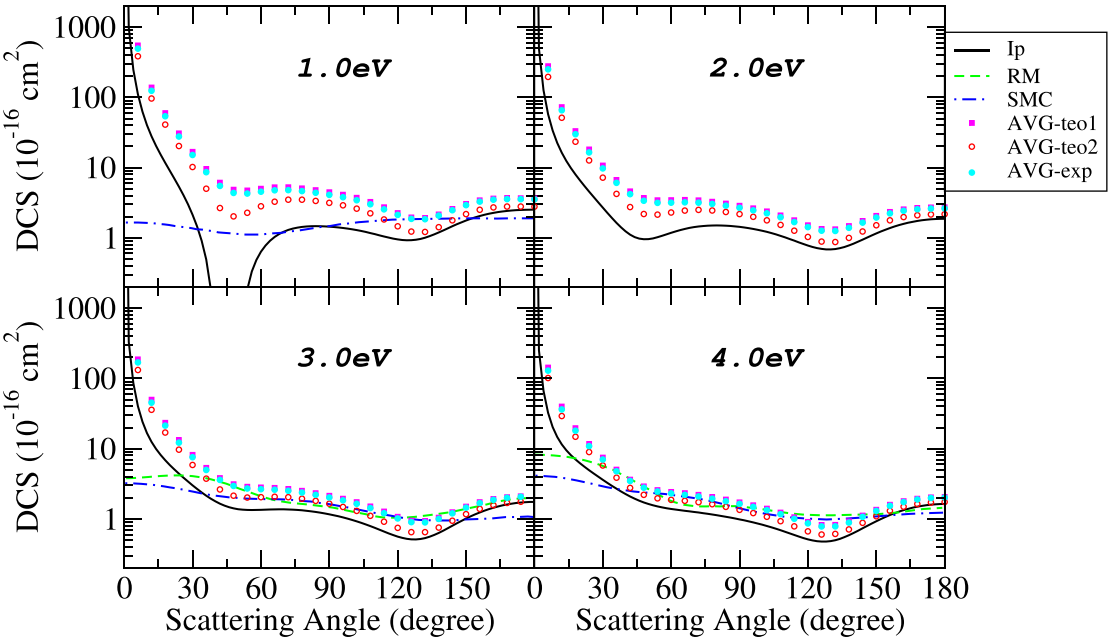

Figure 5. Averaged SEP differential cross sections with Born closure for electron scattering by thermal mixtures of glycine. Comparison between the most stable conformer Ip; RM is calculated by [48] at the SEP level; SMC is calculated by [49] at the SEP level; AVG-teo1 is obtained for a theoretical population of Ip, IIp, IIn, IIIp, IIIn and IVn conformers at 298 K from [29]; AVG-teo2 is obtained for a theoretical population of Ip, IIp, IIIp and IVn conformers at 438 K from [40]; AVG-exp for an experimental population for I, II and III conformers at 443 K from [38]. For impact energies of: 1, 2, 3 and 4 eV.

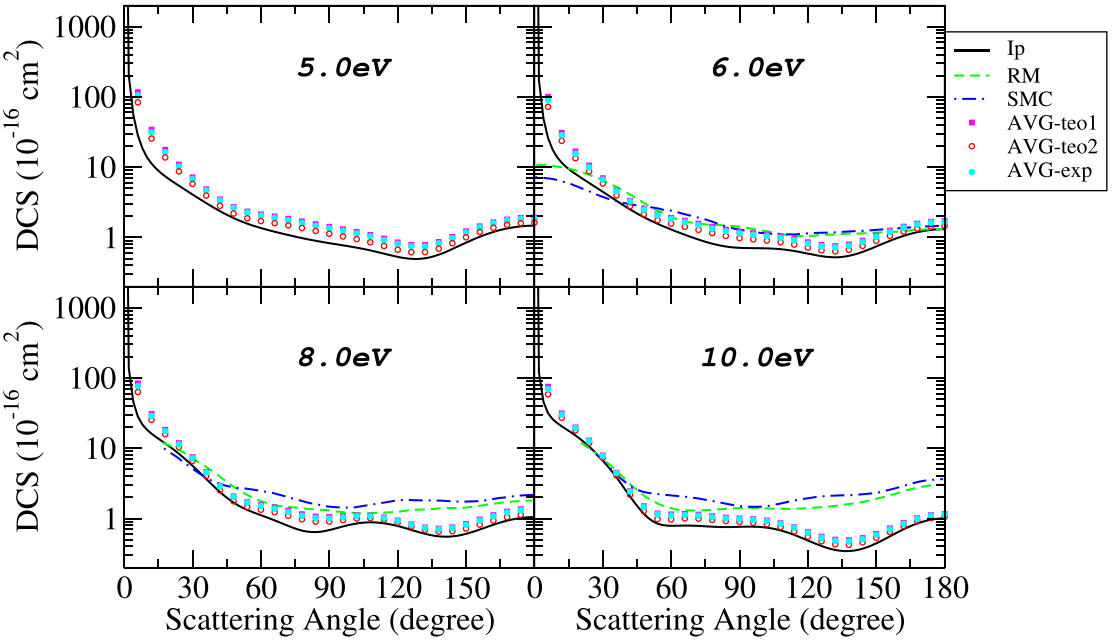

Figure 6. Same as figure 5. For impact energies of: 5, 6, 8 and 10 eV.

IVn conformers calculated by Ke *et al* [29] at temperature of 298 K. The AVG-teo2 theoretical set is deduced from the relative Gibbs free energies calculated by Neville *et al* [40] at 438 K. The experimental population set, AVG-exp, is based on measurements by Stepanian *et al* [38] on glycine vapour at 443 K, who observed only three conformers that they called I, II and III, where we assumed the proportion of 'p' and 'n' for II and III conformers follows the Ke *et al* ratios. The population of conformer II from Stepanian *et al* is very similar to the summed population of IIp and IIn from Ke *et al* (see table 1); the same occurs for the III conformer. That is why there is no significant difference between the AVG-DCS for the AVG-teo1 and AVG-exp population sets even for different temperatures, since IVn contributes only around 3% in the mixture composition. The discrepancy between the lowest energy conformer Ip to the AVG-DCS is more accentuated at

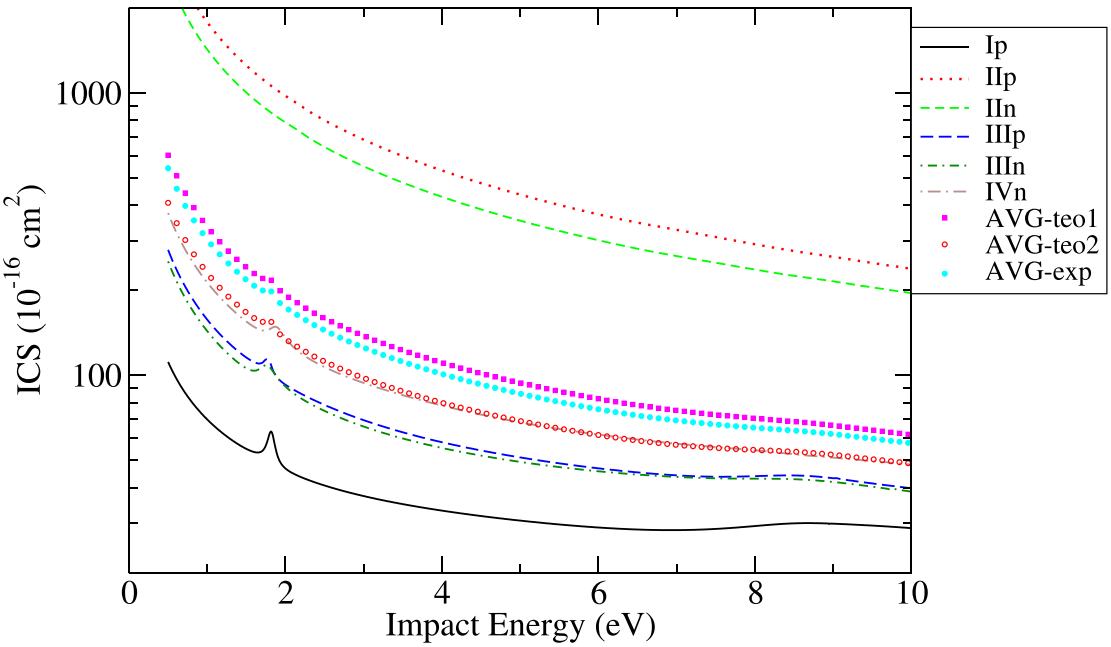

Figure 7. SEP integral cross sections with Born closure for electron scattering for glycine Ip, IIp, IIn, IIIp, IIIn and IVn conformers in gas phase. Comparison also with AVG-teo1 obtained for theoretical population from Ip, IIp, IIn, IIIp, IIIn and IVn conformers at temperature of 298 K [29]; AVG-teo2 obtained for theoretical population from Ip, IIp, IIIp and IVn conformers at 438 K [40] and AVG-exp from experimental population for I, II and III conformers at 443 K [38].

lower impact energies. The AVG-DCS (teo1) is higher than Ip mainly due to the very large DCS of IIp and IIn conformers despite their summed populations is around only 15%. AVG-teo2 is systematically smaller than AVG-teo1 and AVG-exp, mainly because the contribution of conformer IIp is only 9% compared to about 15% (IIp, IIn and II) in the other two sets. In general, the AVG-DCS is not so different from the DCS of conformer Ip as the DCS of Ip is dominant and also because the DCS for all conformers approach to the DCS of conformer Ip as the impact energies increase. Although the DCS for conformers IIp and IIn are still consistently higher than Ip and contribute to increasing the average.

3.4. Integral cross sections

Figure 7 shows the ICS calculated in SEP with Born closure for Ip, IIp, IIn, IIIp, IIIn and IVn glycine conformers. The AVG-ICS are also presented for two theoretical and one experimental populational sets, at 298 K, 438 K and 443 K, respectively. As discussed for the MW spectrum above, for conformers with larger dipole moment have the bigger ICS in electron scattering. The ICS for each conformer is scaled by the dipole moment squared, the magnitude of ICS for IIp>IIn>IVn>IIIp>IIIn>Ip. The lowest energy conformer Ip has the smallest dipole moment of 1.23 D and also has the smallest ICS at all energies studied. The next ICSs in magnitude are for IIIp and IIIn, which have very similar cross sections as are their dipole moments, 2.00 and 1.91 D, respectively. The dipole moments for IIp and IIn conformers are 6.32 D and 5.67 D and also have similar ICS's, however, they are around an order of magnitude larger than the ICS for the conformer Ip. Considering the angular integration of DCS, the ICS is dominated by forward scattering mostly because of the long-range electron-dipole interactions as seen in the figures 3 and 4. The Born closure procedure compute these contributions by including the higher partial waves in the T-matrices. The lower-energy resonance peak near 1.8 eV in the ICS is observed for Ip, IIIp, IIIn and IVn conformers, but is not noticeable for IIp and IIn due to the strong contribution of their large dipole moments in ICS masks the resonance peak. A smoothed resonance peak near 1.86 eV is also observed in the AVG-ICS. In spite of the very large ICS values for conformers IIp and IIn compared with Ip, they contribute around 15% while the lowest energy conformer contributes with more than 62% for the thermal mixture in both population sets (AVG-teo1 and AVG-exp). This means that the AVG-ICS is about 4.8 times bigger than Ip at 1 eV and almost double at 10 eV. It is to be expected that as the impact energy increases the spatial distribution of atoms in the conformers becomes less relevant although the contributions of conformers with very large dipole moments make the averaged cross sections significantly different from the results considering only the lowest energy conformer Ip. The difference between AVG-teo1 and AVG-teo2 in the ICS is around 28% near 1 eV and around 17% near 10 eV. This difference is produced mainly because the population sets give different contributions by the IIp conformer beyond the distinct conformers composition and temperature in the glycine vapour. Therefore, the measurement of elastic cross sections by glycine vapour would be desirable as it would provide more information about the vapour composition and the importance of conformers to the averaged cross sections.

4. Conclusions

In this work we present a theoretical study of electron scattering by glycine molecules in the gas phase. We assume that thermalised glycine vapour at temperatures of 298 K, 438 K and 443 K is mainly populated by up to six conformers of glycine Ip, IIp, IIn, IIIp, IIIn and IVn. An analysis of eigenphase sums shown that all conformers display resonance structures in two regions. The lower-energy resonance usually assigned as the electron attachment to the π^* orbital of CO bond in –COOH group, lie in the range 1.75–2.21 eV depending on the glycine conformer. The higher-energy resonance is broad structure starting above 7.1 eV and discussed in the literature as being related to core-excited shape resonances. In general, an automated fit found further two resonance states for the IIn and IIp conformers, which have very large dipole moments, near 6 D. These additional states could be related to the dipole bound states, since their dipole moments are bigger than the critical value (>1.625 D). The DCS and ICS are calculated for six conformers and compared with averaged DCS and ICS. The comparison between the DCS shown that at lower impact energies the cross sections are more sensitive to the different spatial distribution of atoms in the conformer and with increasing energies the discrepancy reduces.

The AVG-DCS and AVG-ICS are calculated using three population sets. The theoretical population sets are due to the Boltzmann distribution based on the relative Gibbs free energies, one set is for the six conformers at 298 K (teo1) and another is for four conformers at 438 K (teo2). The experimental population set is derived from infrared analysis on matrix isolated glycine vapour at 443 K. This experimental observed only three types of conformers I, II and III, the averaged cross sections calculated by all sets give similar cross sections. However, the AVG-teo2 cross sections are smaller than other AVGs cross sections mainly due to the less contribution of glycine IIp, which has very large dipole moment. The averaged cross sections is significantly different from the lowest energy conformer Ip cross section due to the contribution of conformers with very large dipole moments which have the biggest effect at lower energies. Therefore we suggest that comparisons with measured cross section should really be made with theoretical averaged cross sections when it involves electron scattering with large and flexible molecules, which can generate several conformers; this is particularly important when (some of) these conformers have a large range of dipole moments.

Data availability statement

All data that support the findings of this study are included within the article.

Acknowledgments

M H R acknowledges to Coordenação de Aperfeiçoamento de Pessoal de Nível Superior—Brasil (CAPES) for scholarship Process Number 88882.344196/2019-01; The authors acknowledge computational support of National Supercomputing Centre (CESUP) of Universidade Federal do Rio Grande do Sul (UFRGS) and Scientific Computational Laboratory (LCC) of Physics Department of Universidade Federal do Paraná (UFPR).

ORCID iDs

Jonathan Tennyson https://orcid.org/0000-0002-4994-5238
Milton M Fujimoto https://orcid.org/0000-0003-1780-3750

References

[1] Boudaïffa B, Cloutier P, Hunting D, Huels M A and Sanche L 2000 *Science* **287** 1658–60
[2] Sanche L 2009 *Chem. Phys. Lett.* **474** 1–6
[3] Albrecht G and Corey R B 1939 *J. Am. Chem. Soc.* **61** 1087–103
[4] Tortonda F R, Pascual-Ahuir J L, Silla E and Tuñón I 1996 *Chem. Phys. Lett.* **260** 21–26
[5] Suenram R D and Lovas F J 1980 *J. Am. Chem. Soc.* **102** 7180–4
[6] Iijima K, Tanaka K and Onuma S 1991 *J. Mol. Struct.* **246** 257–66
[7] Császár A G 1992 *J. Am. Chem. Soc.* **114** 9568–75
[8] Ding Y and Krogh-Jespersen K 1992 *Chem. Phys. Lett.* **199** 261–6
[9] Vishveshwara S and Pople J A 1977 *J. Am. Chem. Soc.* **99** 2422–6
[10] Suenram R D and Lovas F 1978 *J. Mol. Spectrosc.* **72** 372–82
[11] Brown R D, Godfrey P D, Storey J W V and Bassez M P 1978 *J. Chem. Soc. Chem. Commun.* **1** 547–8
[12] Sellers H L and Schäfer L 1978 *J. Am. Chem. Soc.* **100** 7728–9
[13] Schäfer L, Sellers H L, Lovas F J and Suenram R D 1980 *J. Am. Chem. Soc.* **102** 6566–8
[14] Lovas F J, Kawashima Y, Grabow J-U, Suenram R D, Fraser G T and Hirota E 1995 *Astrophys. J.* **455** L201
[15] Palla P, Petrongolo C and Tomasi J 1980 *J. Phys. Chem.* **84** 435–42
[16] Dykstra C E, Chiles R A and Garrett M D 1981 *J. Comput. Chem.* **2** 266–72
[17] Millefiori S and Millefiori A 1983 *J. Mol. Struct.: THEOCHEM* **91** 391–3
[18] Siam K, Klimkowski V J, Ewbank J D, Alsenoy C V and Schäfer L 1984 *J. Mol. Struct.: THEOCHEM* **110** 171–82
[19] Ramek M, Cheng V K, Frey R F, Newton S Q and Schäfer L 1991 *J. Mol. Struct.: THEOCHEM* **235** 1–10
[20] Jensen J H and Gordon M S 1991 *J. Am. Chem. Soc.* **113** 7917–24
[21] Yu D, Armstrong D A and Rauk A 1992 *Can. J. Chem.* **70** 1762–72
[22] Hu C H, Shen M and Schaefer H F 1993 *J. Am. Chem. Soc.* **115** 2923–9
[23] Pacios L F, Gálvez O and Gómez P C 2001 *J. Phys. Chem.* A **105** 5232–41
[24] Barone V, Adamo C and Lelj F 1995 *J. Chem. Phys.* **102** 364–70
[25] Nguyen D T, Scheiner A C, Andzelm J W, Sirois S, Salahub D R and Hagler A T 1997 *J. Comput. Chem.* **18** 1609–31
[26] Kaschner R and Hohl D 1998 *J. Phys. Chem.* A **102** 5111–16
[27] Császár A G 1995 *J. Mol. Struct.* **346** 141–52
[28] Miller III T F and Clary D C 2004 *Phys. Chem. Chem. Phys.* **6** 2563–71

[29] Ke H-W, Rao L, Xu X and Yan Y-J 2008 *J. Theor. Comput. Chem.* **07** 889–909
[30] Balabin R M 2009 *Chem. Phys. Lett.* **479** 195–200
[31] Ramek M 1990 *Int. J. Quantum Chem.* **38** 45–53
[32] Sirois S, Proynov E I, Nguyen D T and Salahub D R 1997 *J. Chem. Phys.* **107** 6770–81
[33] Frey R F, Coffin J, Newton S Q, Ramek M, Cheng V K W, Momany F A and Schaefer L 1992 *J. Am. Chem. Soc.* **114** 5369–77
[34] Falzon C T and Wang F 2005 *J. Chem. Phys.* **123** 214307
[35] Godfrey P D and Brown R D 1995 *J. Am. Chem. Soc.* **117** 2019–23
[36] Godfrey P D, Brown R D and Rodgers F M 1996 *J. Mol. Struct.* **376** 65–81
[37] Reva I D, Plokhotnichenko A M, Stepanian S G, Ivanov A Y, Radchenko E D, Sheina G G and Blagoi Y P 1995 *Chem. Phys. Lett.* **232** 141–8
[38] Stepanian S G, Reva I D, Radchenko E D, Rosado M T S, Duarte M L T S, Fausto R and Adamowicz L 1998 *J. Phys. Chem.* A **102** 1041–54
[39] Ivanov A, Sheina G and Blagoi Y 1998 *Spectrochim. Acta* A **55** 219–28
[40] Neville J J, Zheng Y and Brion C E 1996 *J. Am. Chem. Soc.* **118** 10533–44
[41] Aflatooni K, Hitt B, Gallup G A and Burrow P D 2001 *J. Chem. Phys.* **115** 6489–94
[42] Gohlke S, Rosa A, Illenberger E, Brüning F and Huels M A 2002 *J. Chem. Phys.* **116** 10164–9
[43] Scheer A M, Mozejko P, Gallup G A and Burrow P D 2007 *J. Chem. Phys.* **126** 174301
[44] Ptasinska S, Denifl S, Abedi A, Scheier P and Märk T D 2003 *Anal. Bioanal. Chem.* **377** 1115–19
[45] Abouaf R 2008 *Chem. Phys. Lett.* **451** 25–30
[46] Mauracher A *et al* 2007 *Phys. Chem. Chem. Phys.* **9** 5680–5
[47] Gianturco F A and Lucchese R R 2004 *J. Phys. Chem.* A **108** 7056–62
[48] Tashiro M 2008 *J. Chem. Phys.* **129** 164308
[49] dos Santos J S, da Costa R F and Varella M T D N 2012 *J. Chem. Phys.* **136** 084307
[50] Tennyson J 2010 *Phys. Rep.* **491** 29–76
[51] Gillan C J, Tennyson J and Burke P G 1995 *The UK Molecular R-Matrix Scattering Package: A Computational Perspective* (Boston, MA: Springer) pp 239–54
[52] Morrison M A 1988 Near-threshold electron-molecule scattering *Advances in Atomic and Molecular Physics* vol 24, ed D Bates and B Bederson (New York: Academic) pp 51–156
[53] Padial N T, Norcross D W and Collins L A 1981 *J. Phys. B: At. Mol. Phys.* **14** 2901–9
[54] Kaur S, Baluja K L and Tennyson J 2008 *Phys. Rev.* A **77** 032718
[55] Sanna N and Gianturco F A 1998 *Comput. Phys. Commun.* **114** 142–67
[56] Tennyson J, Brown D B, Munro J J, Rozum I, Varambhia H N and Vinci N 2007 *J. Phys.: Conf. Ser.* **86** 012001
[57] Carr J M, Galiatsatos P G, Gorfinkiel J D, Harvey A G, Lysaght M A, Madden D, Mašín Z, Plummer M, Tennyson J and Varambhia H N 2012 *Eur. Phys. J.* D **66** 58–71
[58] Fujimoto M M, Tennyson J and Michelin S E 2014 *Eur. Phys. J.* D **68** 67
[59] Fujimoto M M, de Lima E V R de and Tennyson J 2017 *J. Phys. B: At. Mol. Opt. Phys.* **50** 195201
[60] Tennyson J and Noble C J 1984 *Comput. Phys. Commun.* **33** 421–4
[61] Allan M 2006 *J. Phys. B: At. Mol. Opt. Phys.* **39** 2939–47
[62] Crawford O H 1971 *Mol. Phys.* **20** 585–91
[63] Diken E G, Hammer N I and Johnson M A 2004 *J. Chem. Phys.* **120** 9899–902
[64] Bode B M and Gordon M S 1998 *J. Mol. Graph. Modelling* **16** 133–8